Investigation of heat transfer during magnetohydrodynamic flow of liquid metal in the "pipe in channel" heat exchange system

N. A. Luchinkin[1,2], N. G. Razuvanov[1,2], O. N. Polyanskaya[1,2]

[1] National Research University "Moscow Power Engineering Institute", 111250, Krasnokazarmennaya 17, Bd.1 , Moscow, Russia
[2] Joint Institute for High Temperatures of the Russian Academy of Sciences, 125412, Izhorskaya st. 13 Bd.2, Moscow, Russia

Abstract. Experimental studies of heat transfer during the upward flow of liquid metal in a vertical pipe, located axially inside a square heated channel connected to the natural circulation loop, were carried out. The measurements were performed in the absence and presence of a transverse magnetic field. Measurements both in the inner pipe and in the channel gap were carried out using longitudinal microthermocouple probes. Three main cooling modes are considered for the upward flow of mercury in the pipe and natural convective flow in the channel gap: the natural circulation loop is closed, the loop is opened, and cooling water of the cold leg is on or off. For the case of uniform heating of all sides of the outer channel, average temperature profiles, local heat transfer coefficients distributions, statistical characteristics of temperature fluctuation both in the pipe and in the channel gap were obtained in a wide range of Reynolds and Hartmann numbers. It was found that the flow configuration and its structure in the gap change significantly in the presence of a transverse magnetic field, and also depend on the inclusion of the natural circulation loop.

Introduction

Magnetohydrodynamics (MHD) of liquid metals (LM) is considered in relation to the cooling of fusion reactors. Liquid metals are very attractive coolants for cooling energy-intensive elements of a fusion reactor, such as a blanket or a divertor. Liquid metals have good thermophysical properties: high thermal conductivity and volumetric heat capacity. Due to the high boiling point (unlike water), there is no need to work under high pressure. At the same time, the need to maintain high operating temperatures of the coolant, due to the melting temperature, corrosive activity in relation to structural materials determines the complexity of their operation. Therefore, the international project ITER provides water as the main coolant for blanket and diverter devices. However, the blanket design provides ports for LM modules [1, 2]. Experimental LM modules are being developed for ITER by various project participants, which designed to produce tritium from a lithium in the fusion reactor itself. Lithium is contained both in liquid and in the ceramic backfill forms. Lead and lithium alloys seem to be the most promising coolants in these modules. ITER is a "pure" fusion reactor. Along with such reactors, the development of hybrid fusion-fission reactors is promising. Hybrid fusion-fission reactors are sources of fast neutrons and are designed to produce plutonium from uranium-238 [3]. These relatively small, commercial reactors exclude water as a coolant due to neutron braking. Lead and lead-lithium alloys are chosen here to cool the blanket, where the fissile material is also placed.

The complex geometry of the toroidal chamber, which is surrounded by the first wall and the blanket modules behind it, suggests a complex box-shaped design of the heat exchanger. The box structure will experience severe stress caused by high-energy neutron fluxes, hydrodynamic forces, electromagnetic and thermal stresses. Therefore, tubular heat exchangers are preferred - pipe can withstand heavy loads, both in compression and tension, and in bending. One obvious way to embed a tubular heat exchanger in a blanket box is to fill the space between the tubes and the outer wall of the blanket module with an intermediate medium, also liquid metal. In such a dual cooling system in the pipes, there is a forced flow, where pressure can be raised to ensure the required flow rate, and an intermediate freely convective medium provides heat transfer to the pipes. Such dual schemes are being developed, for example, in the JUST-T project for a hybrid reactor to reduce the activity of spent fuel rods [4].

For heat exchange systems, in addition to hydraulic characteristics, the fields of temperature and distribution of heat transfer coefficients are decisive. Liquid metal heat transfer in such systems applied to fusion reactors has not been sufficiently studied, since it is complicated by electromagnetic interaction. Convective heat transfer is determined both by the laws of MHD and by free-convective phenomena. Such studies were carried out mainly in pipes with mercury coolant. It is difficult to conduct experimental investigations of local characteristics of hydrodynamics and heat transfer using lead loops, due to the high operating temperature and the

relatively high melting temperature. The use of mercury as a model fluid has obvious advantages.

The MPEI and JIHT RAS mercury facilities are combined into a unique MHD complex for studying the hydrodynamics and heat transfer of liquid metals in pipes and channels in longitudinal and transverse magnetic fields (MF). Mercury, a noble metal that is liquid at room temperature, closest in properties to lead, and both belong to the heavy metal class. The low temperatures in the experiment make it possible to use probe methods to study the local characteristics of heat transfer. The upgraded probes made it possible to obtain more detailed, accurate and reliable data on heat transfer.

Detailed three-dimensional measurements using microthermocouple sensors were performed in a series of studies of various configurations of MHD and heat transfer [5]. The results reveal a strong influence of thermogravitational convection (TGC) and external MF, which combined action leads to unpredictable effects that determine the mechanisms of MHD and heat transfer of channel flows, both averaged and pulsating [6]. Numerical modeling of hydrodynamics and heat transfer of experimentally solved problems is also carried out by the methods of RANS [7] and DNS [8]. Using the methods of similarity theory, these data can be transferred to other heat carriers, for example, to lead and its alloys.

In this paper, the subject of study is the "pipe in a channel" cell with a double cooling system, where a forced flow of LM is implemented in the pipe, and free convection is present in the gap between the channel and the pipe. The problem of heat transfer in such a system is complicated by the presence of an external transverse MF, which significantly affects the hydrodynamics of the averaged flow and the pulsation characteristics of the flow.

1 Problem statement and research methodology

The problem of studying heat transfer in the “pipe in a channel” scheme is solved experimentally in a double cooling system at the mercury MHD complex of the MPEI-JIHT RAS. For this purpose, the loop was reconstructed for a new experimental section, which is a vertical stainless steel pipe with an inner diameter of 18 mm, a wall thickness of 1 mm and a length of 1.4 m (Fig. 1). The pipe is inserted into a square channel with a width of 32 mm inside, a wall thickness of 1.5 mm and a length of 1.0 m. At the ends of the channel there are inlet and outlet pipes connected to a natural circulation loop (shown in gray in Fig. 2), which includes a water-cooled heat exchanger 5 and a control valve 9.

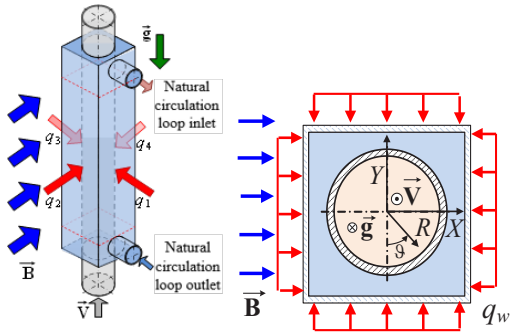

Fig. 1. Scheme of flow and heating.

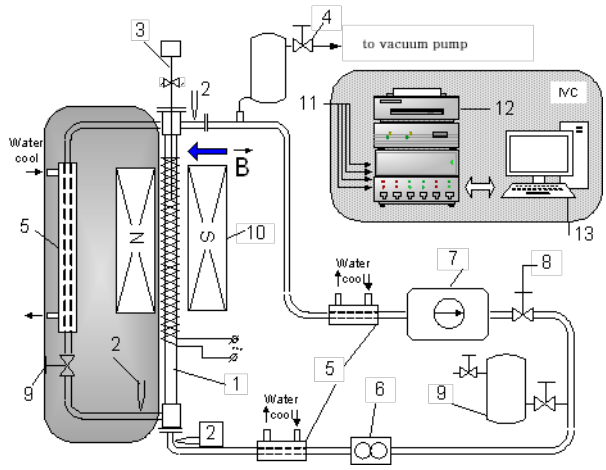

Fig. 2. Experimental loop**.**

An invoice four-section heater made of nichrome tape is mounted on the channel surface, which provides uniform heating of each side of the channel with a heat flux density q_i = const, where i = {1,2,3,4}. Heat flux sensors were mounted in three sections on top of the heater to assess heat losses. The working area and the natural circulation loop are thermally isolated from the environment.

Longitudinal microthermocouple probes 3 are inserted from the end of the working section. A “comb” probe (Fig. 3) is inserted into the pipe, consisting of 9 T-type thermocouples with a junction diameter of 0.2 mm, located along the pipe diameter. The probe could be moved along the length and rotated along the corner of the pipe. This probe makes it possible to obtain three-dimensional fields of average and fluctuation temperature characteristics along the entire length of the heating zone 800 mm long with an accuracy of 0.15 °C. Another longitudinal probe is introduced into the annular space, consisting of 8 thermocouples, which cover a quarter of the channel section: thermocouple 1 is located in the corner, 2 and 3 on the inner sides of the channel wall, 4-6 - on the outer side of the pipe, thermocouples 7 and 8 form a correlation pair serve to measure the longitudinal flow velocity of mercury [9].

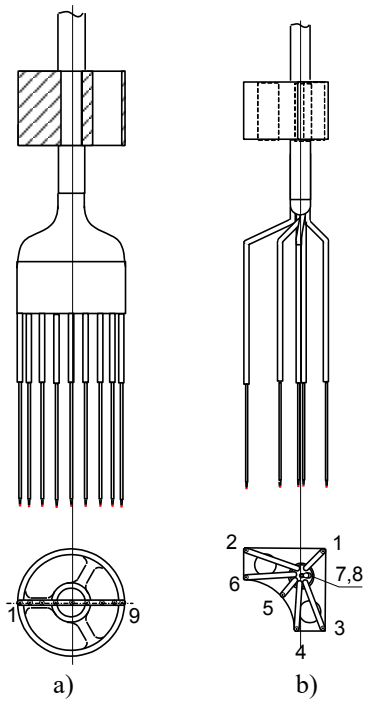

Fig. 3. Longitudinal microthermocouple probes: a) for measuring temperature fields in a pipe, b) for measuring in a channel gap.

Leaving the pipe of the working section, mercury passes through heat exchangers 5, a flow meter with a mercury differential pressure gauge 6 (a vortex flow meter 7 is also embedded in the circuit) and enters an electromagnetic pump 8. The working section is located between the poles of an electromagnet 11, which creates a uniform transverse field over a length of 600 mm in the heating area, starting from 5 gauge.

The loop provides coolant flow rates in the circuit with Reynolds numbers Re up to 85000, heat flux density of heaters in terms of the pipe surface up to 40 kW/m^2 from Grashof number Gr = 10^8, magnetic field up to 1 T with Hartmann numbers Ha = 0-450.

2 Results

On the mercury loop of the MHD complex, the first series of experiments were carried out to measure the temperature fields and heat transfer characteristics during an upward flow of mercury in a pipe placed in a square channel filled with mercury connected to a natural circulation loop. The experiments were carried out with two probes: in the pipe with a longitudinal probe of the "comb" type, then with the second probe in the gap between the pipe and the channel.

The heating mode was set close to homogeneous, when all 4 sides of the channel had the same heat flux with a density $q_c = q_1 = q_2 = q_3 = q_4$ of the pipe equal to 30 kW/m^2 in terms of the inner wall of the pipe. The regime parameters were varied by the Reynolds numbers, determined by the flow rate in the pipe, and by the Hartmann numbers, determined by the magnetic field induction also in the pipe. The measurements were carried out along the length with a step of 5 d at a fixed angle (0 and 90°) and in some sections along the angle with a step of 15°. At each measurement, samples of temperature values of length 60 were taken at a frequency of 100 Hz for each thermocouple of the probe. Based on the results of the sample, the mean value was calculated, the standard deviation is the variance. The measurements were repeated in three main modes: mode I - the cooling loop is closed, convective movement occurs only in the space between the pipe and the channel, mode II - the cooling loop is open without cooling, mode III - the cooling loop is open with cooling.

Consider the results of measurements obtained in the pipe.

The fields of the averaged temperature (Fig. 4), the fields of temperature fluctuations intensity and temperature fluctuations near the wall (Fig. 5) are shown. The intensity of temperature fluctuations is defined as the square root of the dispersion σ. Measurements in modes without a magnetic field (Ha = 0) showed that the field of averaged temperature (Fig. 4a) and pulsating (Fig. 5a) is almost axisymmetric, despite the fact that the geometry of the "pipe in a channel" system does not have axial symmetry. No axial symmetry is observed in a magnetic field (Fig. 4b). The pulsating temperature-intensity field changes much more strongly (Fig. 5). The level of temperature fluctuations generally decreases and the intensity distribution in the transverse MF takes on a saddle shape (Fig. 5b) with maxima near the walls perpendicular to the magnetic field.

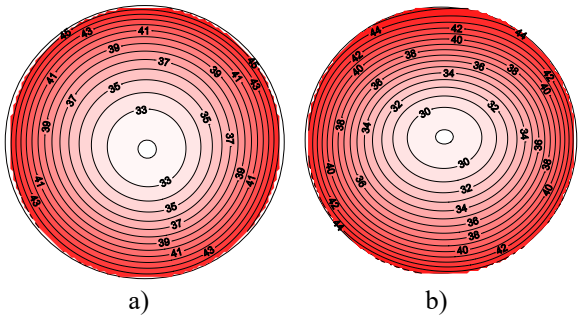

Fig. 4. Temperature fields in the pipe section z/d = 37, Re = 50000, q_w = 30 kW/m^2, natural circulation loop closed: a) Ha = 0, b) Ha = 470.

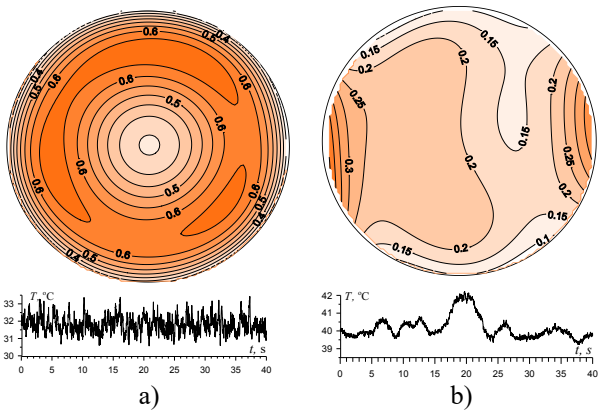

Fig. 5. Temperature fluctuations intensity fields and characteristic pulsations near the wall (X = -1,Y = 0) in the pipe section z/d = 37, Re = 50000, q_w = 30 kW/m^2, natural circulation loop closed: a) Ha = 0, b) Ha = 470.

Examples of fluctuation temperature oscillograms near one of these points are also shown. Without a magnetic field, the nature of the signal is turbulent; in the MF, high-frequency harmonics are practically suppressed, the signal becomes low-frequency, but in amplitude not lower than the turbulent level.

The change in hydrodynamics in the MF is well illustrated by numerical simulation data, which are also performed by the authors. The calculation model based on the averaged equations of magnetohydrodynamics, corresponding to the experimental conditions, is described in detail in [13]. The calculation was carried out in ANES [11], where the low-Reynolds k-ε - Launder-Sharma turbulence model [12] was used, taking into account the suppression of turbulence by the transverse MF [13]. Typical examples of the results are shown in Figs. 6.

The calculated data in the channel section in Fig. 6(a and c) show that the velocity and temperature fields without MF are practically axisymmetric.

In a transverse MF (Fig. 6 b and d), the velocity fields change strongly: the axial symmetry disappears, and due to the Hartmann effect [14], the velocity profiles along the MF along the horizontal axis flatten. In the calculation, the electrical conductivity of the walls was set, which was reduced by a factor of 30 compared to the tabular data for stainless steel AISI 321. So that the walls turn out to be weakly conductive, which, in general, corresponded to the experimental conditions due to the presence of an oxide film and deposits. In addition, an upward flow occurs in the gap between the pipe and the channel walls in the X-Z axial plane. These flows are associated with the generation of an electric current and the appearance of an electromagnetic force (Ampère force) near the walls perpendicular to the MF induction.

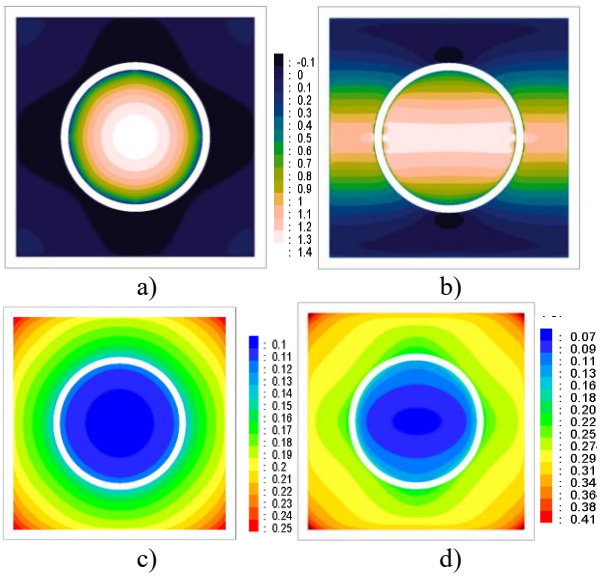

Fig. 6. Calculated fields of the longitudinal velocity component a) and b) and dimensionless temperature c) and d) in the pipe section z/d = 36, Re = 20000, q_w = 30 kW/m^2, natural circulation loop closed: a) и b) Ha = 0, c) и d) Ha = 450.

Since the calculation is presented for mode I with a closed loop of natural circulation, a downward flow is observed in the region of the walls parallel to the MF. That is, there is a circulation of liquid metal in the gap. A completely different structure of secondary flows in the absence of MF in Fig. 6 a. Here, ascending flows arise in the corner regions of the channel and downward flows between them near the pipe walls. Such a flow structure in the pipe and in the square channel determines the shape of the temperature fields and the temperature distribution of the wall in the pipe along the section perimeter, which is illustrated by the graphs in Figs. 8. Here are the distributions of the dimensionless wall temperature θw along the length of the pipe for two modes: with an opened and a closed loop. For comparison, the graphs show the values of 1/NuT and 1/Nulam,Ha, calculated: for a developed turbulent flow according to the Lyon formula NuT = 7 + 0.025Pe$^{0.8}$ and for a stabilized laminar flow in a transverse MF, taking into account the Hartmann effect Nulam, Ha=7 [14].

In the case of a closed loop (Fig. 7a), the experimental points in the absence of MF turn out to be higher than the turbulent values, being located between the dependences 1/NuT and 1/Nulam,Ha. In the transverse MF with an increase in the Hartmann number. The wall temperature rises slightly, reaching laminar values 1/Nulam,Ha. It is interesting that in the case of the maximum MF in the experiment (Ha=460), the distribution has two maxima and two minima, which is associated precisely with the structure of the MHD flow explained above by the numerical calculation data: near the points with angles of 0 and 180°, normal to the MF, the heat transfer increases due to intense generation of flows flow from these two sides of the pipe.

In mode II (with an open loop) in fig. 7(b), heat transfer is significantly improved due to the circulation of LM along the channel, and the wall temperature decreases, both in the MF and without it. In the absence of MF (Ha=0), the temperature on the wall is practically at the turbulent level 1/NuT. In mode III, where natural circulation loop cooling is added, temperatures are further reduced, not shown in the figure.

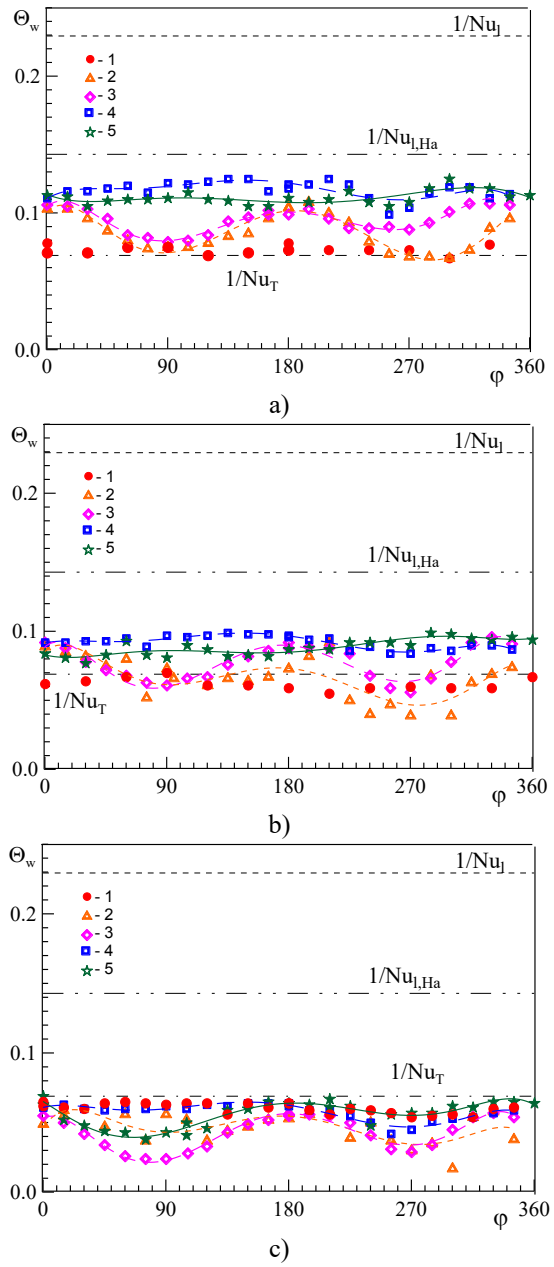

Fig. 7. Distribution of the dimensionless wall temperature Θ_w along the perimeter of the pipe section Re = 50000, q_w = 30 kW/m^2: a) mode I, b) mode II, c) mode III (1 – Ha = 0, 2 - 100, 3 - 200, 4 - 350, 5 - 470).

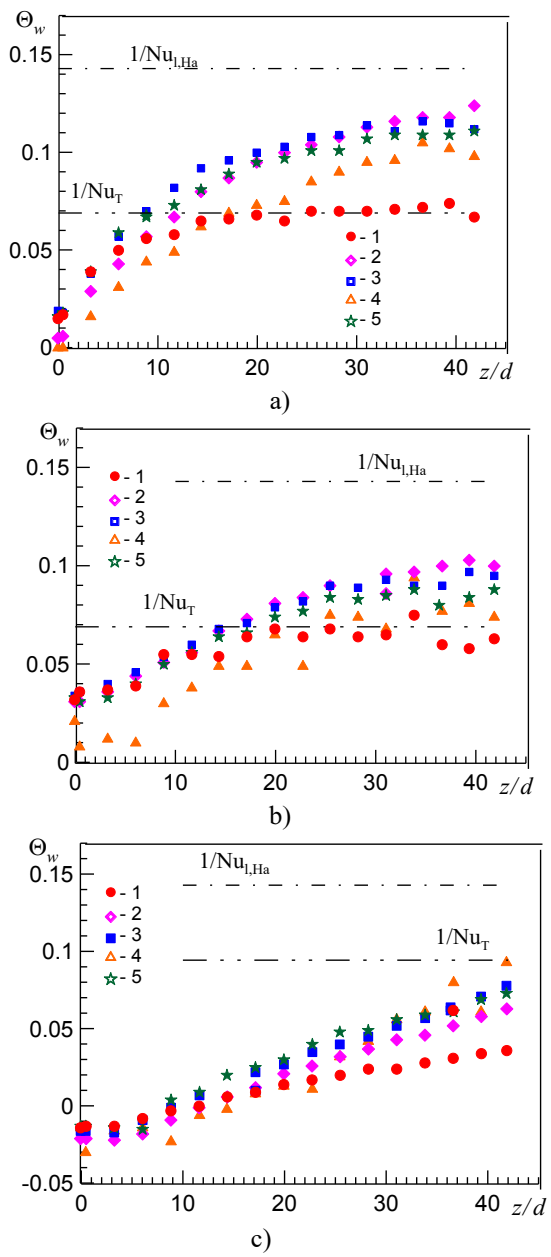

Fig. 8. Distribution of the dimensionless wall temperature Θ_w along the length of the pipe (φ = 90°) Re = 20000, q_w = 30 kW/m^2: a) mode I, b) mode II, c) mode III (1 – Ha = 0, 2 - 100, 3 - 200, 4 - 350, 5 - 470).

All three circulation modes are shown in the graphs of the wall temperature distribution along the length of the pipe in Fig. 8. Temperatures (in the plane φ=90o), starting from the entrance to the heating zone, grow monotonously, reaching a constant level, reaching stabilization. These results make it possible to judge the length of the initial thermal region, which takes from 10 to 20 calibers in Fig. 8 a. and b. That is, they occupy a significant part of the heating zone. In modes with high Reynolds numbers, the initial thermal section can occupy the entire length of the working section heating.

In mode III (Fig. 8c), no thermal stabilization is observed and the temperatures on the wall increase monotonically. It is noteworthy that the temperature level is noticeably lower than in modes I and II, which is quite natural, since in this mode ~35% of heat is removed in the natural circulation loop.

Of particular interest are the results of temperature measurements in the channel gap, which are shown below in Fig. 9–11. On fig. 9b mode I shows the distributions of the dimensionless wall temperature □c determined by the mass average temperature and the pipe diameter. Obviously, the maximum temperature is at the corner point of the channel (shown by blackened round dots 1) and is 2–2.5 times higher than the temperature on the outer wall of the pipe (points 4–6). The temperatures on the channel wall in the middle in the axial planes X = 0 and Y = 0 (points 2-3) lie between them. In the presence of an MF (Fig. 9b), all temperatures increase somewhat, which is a consequence of the suppression of turbulence and laminarization of the flow in the gap.

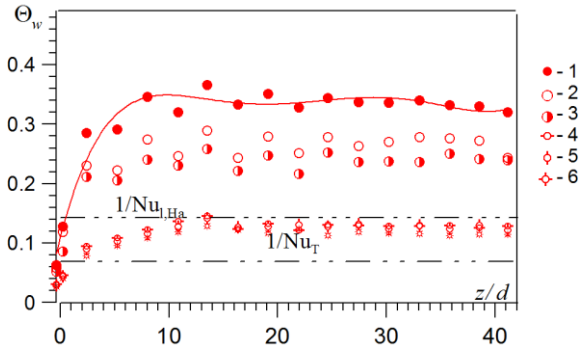

a)

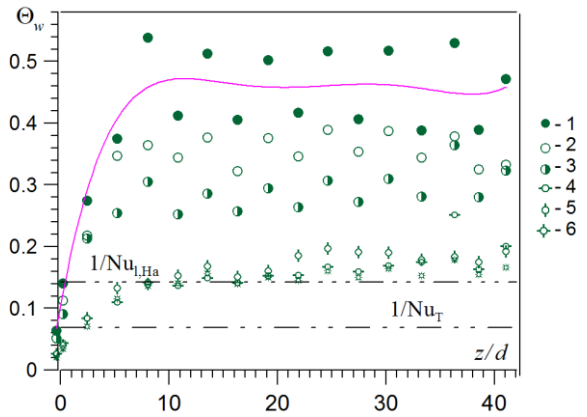

b)

Fig. 9. Distribution of the dimensionless wall Θ_w along the length of the channel gap in mode I, Re = 50000, q_w = 30 kW/m^2: a) Ha = 0, b) 460: 1 - in the corner of the channel, 2 - on the inner wall of the channel X = 0 and 3 -Y = 0, 4 - on the outer wall of the pipe X = 0, 5 - between 4 and 6, 6 - on the outer wall of the pipe Y = 0.

Similar results are shown for regime II with an open loop of natural circulation (Fig. 11). The behavior of the data is the same as in the case of mode I, but the temperature level is somewhat reduced. Temperatures are significantly reduced in mode III (Fig. 12), when the loop operates with cooling. Some temperature oscillations around solid curves, noticeable for temperatures on the inner sides of the channel walls, are apparently related to the imperfect design of the heaters.

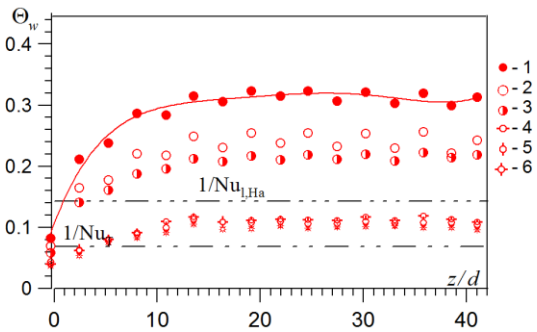

a)

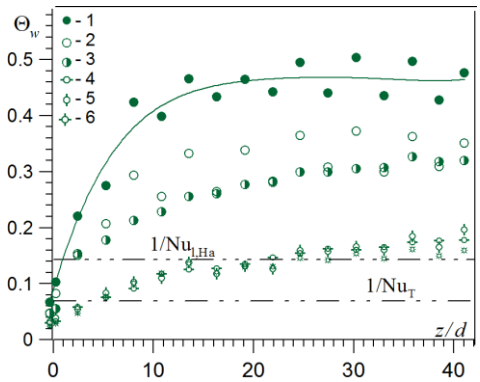

b)

Fig. 10. Distribution of the dimensionless wall Θ_w along the length of the channel gap in mode II, Re = 50000, q_w = 30 kW/m^2; a) Ha = 0, b) 460: 1 - in the corner of the channel, 2 - on the inner wall of the channel X = 0 and 3 -Y = 0, 4 - on the outer wall of the pipe X = 0, 5 - between 4 and 6, 6 - on the outer wall of the pipe Y = 0.

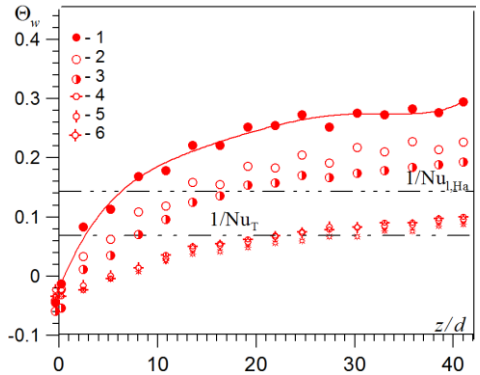

a)

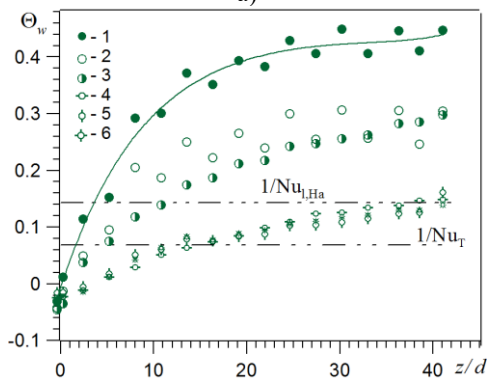

b)

Fig. 11. Distribution of the dimensionless wall Θ_w along the length of the channel gap in mode III, Re = 50000, q_w = 30 kW/m^2: a) Ha = 0, b) 460: 1 - in the corner of the channel, 2 - on the inner wall of the channel X = 0 and 3 -Y = 0, 4 - on the outer wall of the pipe X = 0, 5 - between 4 and 6, 6 - on the outer wall of the pipe Y = 0.

Of particular interest are the primary data of signals from sensor thermocouples in the channel gap. Typical oscillograms are shown in Figs. 12-13 for modes II and III, for all longitudinal probe thermocouples. The shape of the signal in modes without MF indicates the turbulent nature of the free convective flow in the channel gap. The amplitude of oscillations (in the flow in the graphs of Fig. 12-13 c) is here 2 times higher than in the pipe, where the LM flow is forced.

In the MF, the signal strongly changes in shape: due to the suppression of turbulence, the nature of the signal becomes low-frequency with smooth intense oscillations lasting 5–10 s. These fluctuations are associated with the instability of free convective currents caused by both buoyancy forces and electromagnetic forces. These vibrations penetrate well into the wall of the channel and pipe.

Low-frequency temperature fluctuations in the MHD LM flow were found by us repeatedly in studies in pipes and channels in various flow configurations with respect to gravity and MF direction. We explained these pulsation effects by the development of large-scale vortex structures in the flow caused by thermogravitational convection, which are selectively (with axes parallel to the magnetic field induction) formed and stabilized in the LM flow by a strong external magnetic field against the background of suppression of homogeneous small-scale turbulence.

The danger of intense temperature pulsations for real heat-exchange LM systems was noted, which, given their low-frequency nature, easily penetrate the wall, causing additional alternating thermal stresses.

As can be seen, in the present study, these phenomena are also found in the "pipe in the channel" system. The exception is mode III, when the natural circulation loop operates with cooling. At the same time, practically no turbulent pulsations are observed in the transverse MF (Fig. 13, b, d, f): the flow regime in the annular gap is laminar.

A pair of thermocouples 7 and 8, as already mentioned, represents a correlation pair and makes it possible to measure the average longitudinal velocity component V_z in the gap at the point $\varphi = 45^o$ and $R = r/r_0 = 1.4$ using the correlation method [9]. We estimated the velocity measurement uncertainty as 7%. In mode I, the loop is closed, there is no circulation in the circuit and the speed is not determined. On the contrary, in mode II in Fig. 14, referred to the average speed of the forced flow in the pipe (v_0 = 0.31 m/s), the speed is recorded and amounted to $V_z = v_z/V_0 = 0.09$ in the absence of MF (Ha = 0) and in presence of MF: $V_z = 0.10$ (Ha = 100), $V_z = 0.035$ (Ha = 200), $V_z = 0.027$ (Ha = 340), $V_z = 0.029$ (Ha = 450). In mode III (loop open with cooling) in fig. 14, the flow rate increased markedly - $V_z = 0.17$ (Ha = 0), in the absence of MF and in the presence of MF: $V_z = 0.14$ (Ha = 100), $V_z = 0.15$ (Ha = 200), $V_z = 0.09$ (Ha = 340), $V_z = 0.085$ (Ha = 450). It must be understood that the local speed in the gap between the pipe and the channel can differ greatly from the average, that is, this is not the circulation speed in the circuit. In a transverse MF, the velocity distribution over the cross section and the flow structure change strongly: first of all, homogeneous small-scale turbulence is suppressed, and only large-scale inhomogeneities carry information about the velocity. Therefore, the apparent decrease in the measured local velocity in the MF with an increase in the Hartmann number should not be surprising.

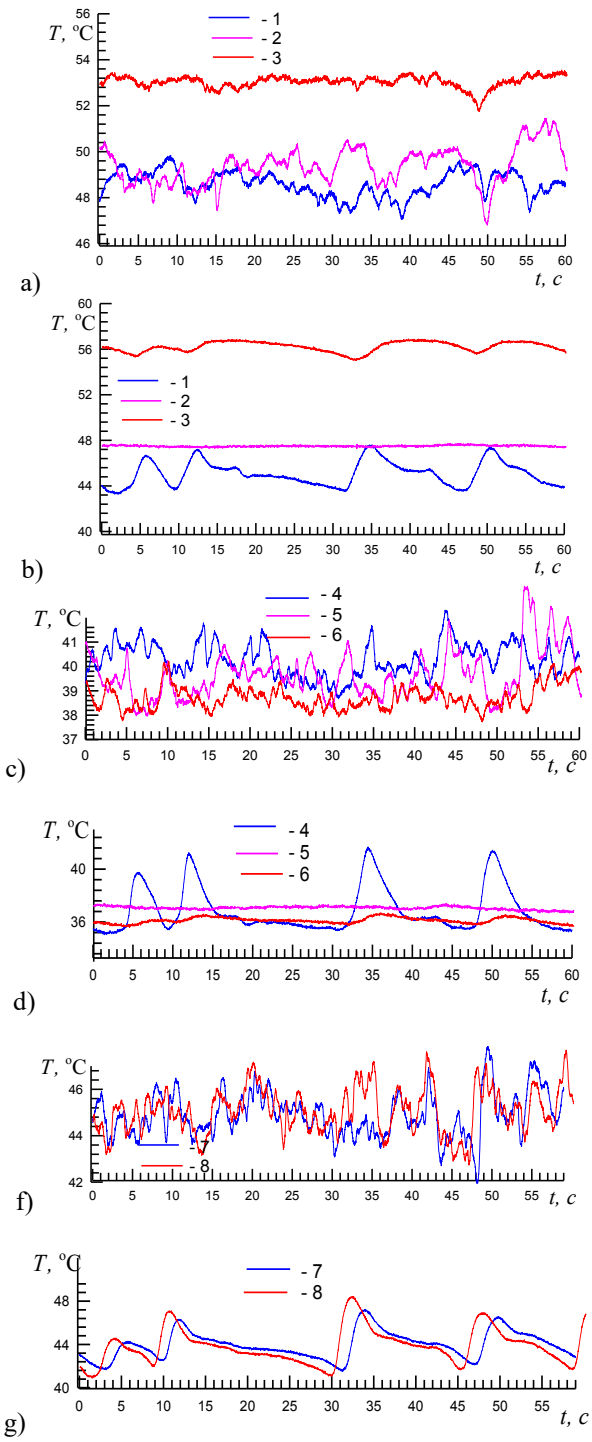

Fig. 12. Examples of temperature signals in mode II in the pipe section z/d = 37, Re = 50000, q_w = 30 kW/m^2, Ha = 0 (a, c, f) and Ha = 340 (b, d, g): a,b) on the inner wall of the channel X = 0 (1) and Y = 0 (2) and in the corner of the channel (3), c,d) on the outer wall of the channel pipe X = 0 (4) and Y = 0 (5) and at the point between them (6), f,g) correlation pair in the flow (7, 8).

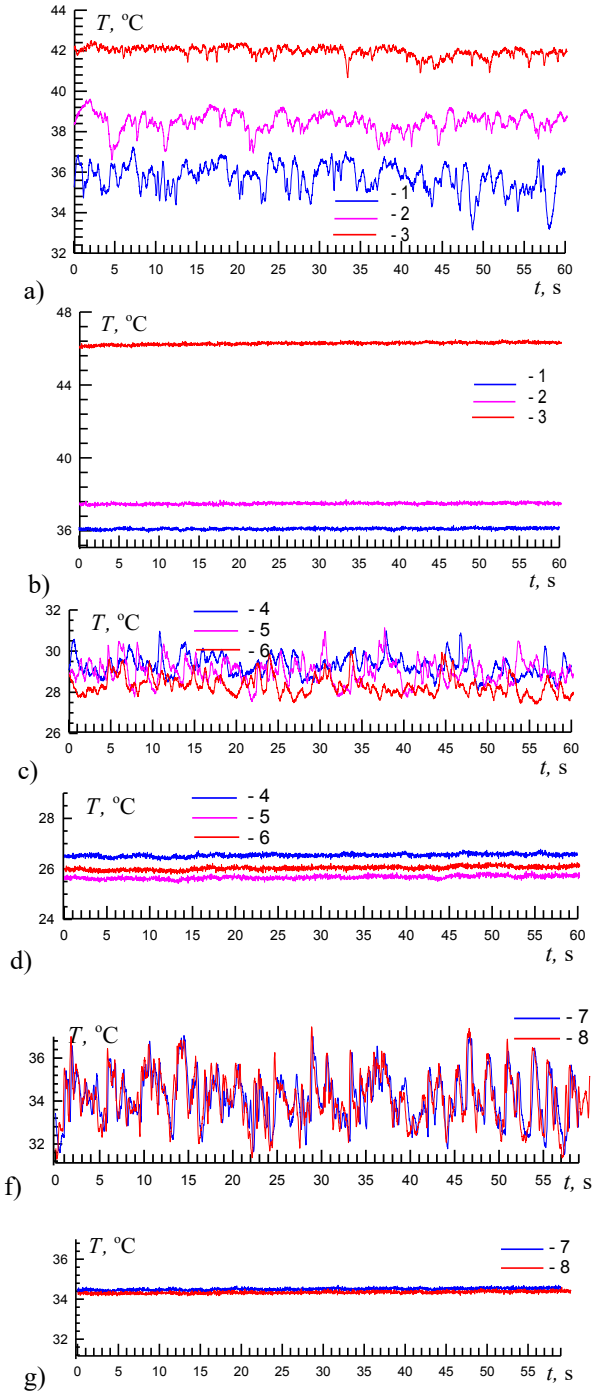

Fig. 13. Examples of temperature signals in mode II in the pipe section z/d = 37, Re = 50000, q_w = 30 kW/m^2, Ha = 0 (a, c, f) and Ha = 340 (b, d, g): a,b) on the inner wall of the channel X = 0 (1) and Y = 0 (2) and in the corner of the channel (3), c,d) on the outer wall of the channel pipe X = 0 (4) and Y = 0 (5) and at the point between them (6), f,g) correlation pair in the flow (7, 8).

In general, heat transfer from the case of lifting flow in a "clean" pipe to the "pipe in a channel" system in modes I, II and III is consistently improved as in the absence, in a transverse MF.

Convection in the gap between the walls of the channel and the pipe filled with LM as a whole improves the heat transfer in the pipe. This is evidenced by the Nusselt numbers $\mathrm{Nu} = 1/\overline{\Theta_w}$ calculated from the wall temperature, averaged over the perimeter of the pipe section, remote from the entrance to the heating zone at a distance of z/d=36 and in the region of a homogeneous MF, depending on the Peclet number Pe. The graphs (Fig. 14) also show the dependencies NuT, $\mathrm{Nu}_{lam,Ha}$ и Nu_{lam}=4.36. It can be seen from the graphs for regime I that, in the absence of MF, the experimental points are located near the Lyon curve, and a certain decrease in heat transfer is associated with the general laws of heat transfer during mixed convection with an upward flow [15]. We also observed a more significant decrease in heat transfer in the case of an upward flow in a separate pipe with uniform heating [16]. It also shows the error corridor, which was 5-10% depending on Re (Pe).

The situation with heat transfer improves in mode II, when the natural circulation loop is in operation and the Nusselt numbers increase both without MF and in the transverse MF.

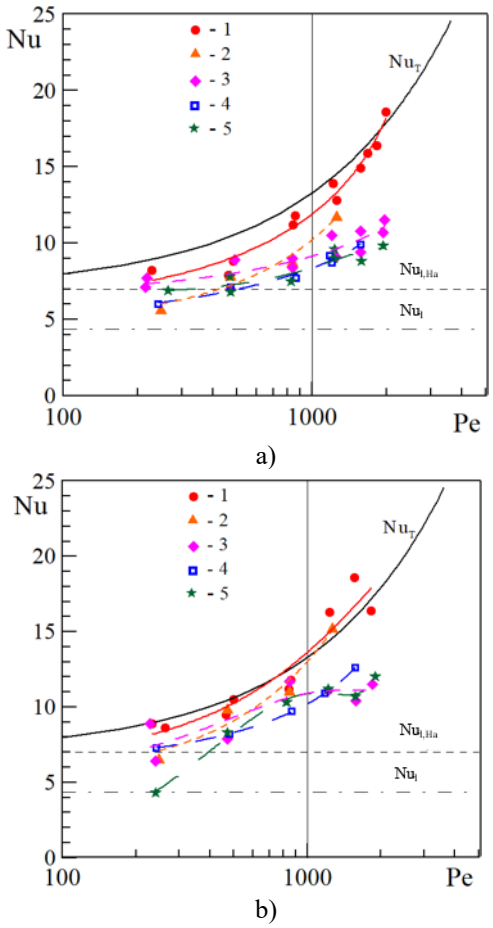

Fig. 14. Dependence of the Nusselt number Nu on the Peclet number Pe, qw = 30 kW/m^2: a) mode I, b) mode II (1 – Ha = 0, 2 – Ha = 10, 3 – Ha = 200, 4 – Ha = 340, 5 – Ha = 470).

Conclusion

The first studies of heat transfer with a forced flow of mercury in a vertical pipe inserted into a square-section channel filled with mercury ("pipe in a channel" scheme) connected to a natural circulation loop were carried out. At this stage, the upward flow in the transverse MF and uniform heating of all four channel walls were considered. Similar conditions are possible

in the LM cell of the tubular module of the fusion blanket.

Three main modes of cooling are considered: when the loop is closed, when the loop is open for the circulation of LM in the gap without cooling and with cooling. As a result of probe measurements of temperature fields and heat transfer characteristics, for the first time an array of data was obtained in the range of Re numbers from 10000 to 85000, with the Grashof number Gr $=10^8$, in the transverse MF up to 1 T with Hartmann numbers Ha = 0-470. It was found that natural convection occurs in the gap under experimental conditions as a result of the action of buoyancy and electromagnetic forces. The configuration of the flow and its structure in the gap essentially depend on the presence of a transverse MF, as well as on the inclusion of a natural circulation loop and its cooling. Gap convection improves heat transfer in the pipe-in-duct system under study to a greater extent when the natural circulation loop is turned on and to the greatest extent when it is additionally cooled. The structure of natural convective flows in the absence of MF in the gap has a turbulent character, and in the presence of a transverse MF it changes significantly. On the one hand, the MF suppresses small-scale turbulence, and on the other hand, it leads to additional instability and the appearance of very low-frequency temperature fluctuations that penetrate the walls of the channel and pipe. The maximum temperature in all modes was observed in the corners of the channel.

The most advantageous from the point of view of heat exchange efficiency is the mode of operation with a natural circulation circuit with cooling. In this case, the temperature is significantly reduced both in the pipe and in the gap between the channel and the pipe, and the flow in the transverse MF becomes more stable - purely laminar.

The data obtained in the experiments will serve as the basis for testing the performance of computational numerical models of such cooling systems.

This work was supported by the Ministry of Science and Higher Education of the Russian Federation (State Assignment No. 075-01129-23-00).

References

1. ITER Organization. Annual report (2013)
2. D. Yurov, V. Prikhod'ko, Physics-Uspekhi, **57**, 11 (2014)
3. J. Aubert, G. Aiello, N. Jonqures, A. Li Puma, A. Morin, G. Rampal, Fusion Eng. Des., **89**, (2014)
4. L. Bühler, C. Mistrangelo, Fusion Eng. Des, **124**, (2017)
5. O. Zikanov, I. Belyaev, Y. Listratov, P. Frick, N. Razuvanov, V. Sviridov, Appl. Mech. Rev., **73**, 1 (2021)
6. I. Belyaev, P. Frick, N. Razuvanov, E. Sviridov, V. Sviridov, Int. J. Heat Mass Transfer, **127** (2018)
7. I. Belyaev, D. Biryukov, N. Pyatnitskaya, N. Razuvanov, E. V.Sviridov, Therm. Eng, **66**, 6 (2019)
8. V. Sviridov, N. Razuvanov, Yu. Ivochkin, Ya. Listratov, E. Sviridov, L. Genin, V. Zhilin, I. Belyaev, *Liquid metal heat transfer investigations applied to tokamak reactor*, in Proceeding of the International Heat Transfer Conference — IHTC14, 8-13 August 2013, Washington, DC, USA, (2010)
9. O. Zikanov, I. Belyaev, Y. Listratov, P. Frick, N. Razuvanov, V. Sviridov, Appl. Mech. Rev., **73**, **(**2021)
10. N. Luchinkin, N. Razuvanov, I. Belyaev, V. Sviridov, High Temp, **58** (2020)
11. V. Artemov, G. Yan'kov, V. Karpov, M. Makarov, Therm. Eng, **47**, 7 (2000)
12. B. Launder, B. Sharma, Letters Heat Mass Transfer, **1 (**1974)
13. N. Pyatnitskaya, I. Melnikov, N. Razuvanov, A. Novikov, E. Sviridov, Magnetohydrodynamics **55**, 1-2 (2019)
14. J.Hartmann, Mat-Fys. Medd.Kgl. Danske vid selskab, **15**, 6 (1937)
15. B. Petukhov, A. Polyakov, Nauka Press (1986)
16. N. Luchinkin, N. Razuvanov, P. Sardov, O. Polyanskaya, J. Phys: Conf. Series, **2057**, 1(2021)